# Image-Rejection Up-/Down-Converter LO Distribution Chain for 5G mm-wave Phased-Array Systems

Aniello Franzese [1], Nebojsa Maletic [1], Renato Negra [2], and Andrea Malignaggi [1]

[1]IHP – Leibniz-Institut für innovative Mikroelektronik, Im Technologiepark 25, 15236 Frankfurt (Oder), Germany
[2]Chair of High Frequency Electronics - RTWH Aachen, Kopernikusstr. 16, 52074 Aachen, Germany

***Abstract*—This paper reports on a local-oscillator (LO) distribution chain suitable for 5G mm-wave image-rejection up-/down-converter. The chain consists of a single-ended-to-differential active converter, which achieves low phase and amplitude imbalance, minimizing the area occupation. Secondly, a frequency doubler is included in the frontend. Following, buffer amplifiers boost the second-harmonic amplitude extracted from the doubler, and a differential polyphase quadrature filter generates two I/Q couples of differential signals, such that four signals can feed two up- or down-converter mixers to achieve sideband suppression for up-conversion operations or image-rejection for down-conversion, respectively. The LO chain is suitable to be provided with an input signal ranging from 11.5 to 13.5 GHz and achieving outputs from 23 to 27 GHz with quadrature capabilities. Finally, the maximum single-ended saturated output power is −1 dBm at 26 GHz and stays above −3.2 dBm for the entire band.**

***Index Terms*—5G, image-rejection, sideband, up-converter, down-converter, mixer, LO**

## I. Introduction

The fifth-generation mobile communications (5G) introduces phased antenna arrays (PhAAs) for data transfer. These PhAAs generate beams which can be steered, pointing to the final user, and thus increasing the spectral efficiency. The data transfer can make use of several beamforming techniques. However, an agile beamforming method is done in the analogue domain, where the correct phase to the antenna element is generated in the radio frequency (RF) frontend. Nevertheless, the intermediate frequency (IF) signal should be up- or down-converted using a local oscillator (LO) [1]–[3]. Moreover, routing on-board high-frequency LO signals faces several impairments, *i.e.*, losses. Therefore, the authors propose a low LO frequency, which is multiplied and amplified on the chip. This way, the on-board routing is straightforward and decreases the power dissipation. On top of that, up- and down-converter circuits should rely on the precise generation of in-phase (I) and quadrature (Q) signals to cancel the image frequency for down-conversion or suppress one sideband signal for up-conversion. Fig. 1 shows a possible architecture of the aforementioned converters. The work in this article describes the distribution of a quadrature LO chain with low phase and amplitude imbalance. As shown in Fig. 1, the chain is made of an active single-ended-to-differential converter (balun) which feeds a differential doubler. Then, a polyphase quadrature filter (PPF) generates the differential I and Q LO signals. These two signals are amplified and then routed to a second buffer amplifier before feeding the mixers (not part of this work) for both up- and down-conversion. The LO at the mixer input should achieve low phase and amplitude imbalance. Therefore, an analysis of the PPF imbalance is necessary.

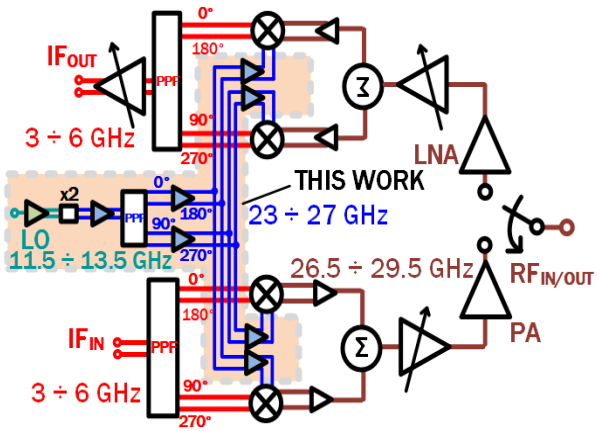


Fig. 1. Diagram of an up-/down-converter architecture and the proposed work.

## II. Circuit Analysis

An ideal LO distribution chain should provide balanced quadrature signals with equal amplitude. Indeed, phase and amplitude imbalance will reduce image-rejection or sideband suppression, degrading the transceiver performance. The image-rejection ratio ($IMRR$) is a figure-of-merit (FOM) of an LO chain [4] and can be quantified using

$$IMRR = \frac{1 + 2\Delta a \cos(\Delta\theta) + \Delta a^2}{1 - 2\Delta a \cos(\Delta\theta) + \Delta a^2}, \quad (1)$$

This work was partially supported by the European Commission and the German Federal Ministry of Education and Research (BMBF) under the contract No. 737454-ECSEL TARANTO.

2023 IEEE Radio and Wireless Symposium (RWS) | 978-1-6654-9344-4/23/$31.00 ©2023 IEEE | DOI: 10.1109/RWS55624.2023.10046204

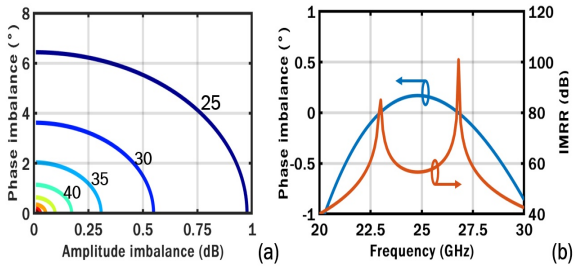


Fig. 2. (a) IMRR in dB as a function of the amplitude and phase imbalance, and (b) IMRR and phase imbalance of the PFF across the frequency.

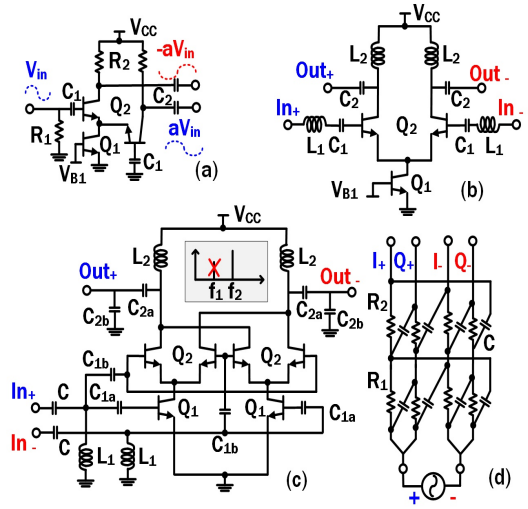


Fig. 3. Schematic of (a) input active balun, (b) buffer amplifier, (c) doubler, and (d) polyphase filter.

where $\Delta a$ denotes the amplitude imbalance, and $\Delta\theta$ is the phase imbalance. Fig. 2(a) shows the $IMRR$ as a function of the two parameters. A Type-II two-stage PPF [5] has been selected for this work to keep the phase imbalance low for a reasonable bandwidth and because of its ideal amplitude balance. Hence, only phase contributes to the $IMRR$ are considered for this analysis. Indeed, the $IMRR$ for this kind of PFF is expressed as

$$IMRR_{PPF} = \cot^2\left(\arctan 0.5\left(wA - \frac{1}{wA}\right)\right), \quad (2)$$

where $A = (w_1+w_2)/(w^2+w_1w_2)$. Moreover, $w_1 = 1/R_1C_1$ and $w_2 = 1/R_2C_2$ are the two resonant frequencies of the PPF. Fig. 2(b) shows the phase imbalance and the $IMRR$ of the designed PPF. In the same frequency range, the corresponding $IMRR$ is better than 50 dB. Even though the PPF has a constant amplitude behaviour, amplitude imbalances can come from other circuit blocks, *e.g.*, amplifiers at the outputs of the PPF. Indeed, they can exhibit imbalance due to process, voltage, and temperature (PVT) variations.

## III. Circuit Design

The LO chain is made of three active components and a PPF. The buffer amplifiers are used before and after the PPF to enhance the gain and restore the phase. Seven of these

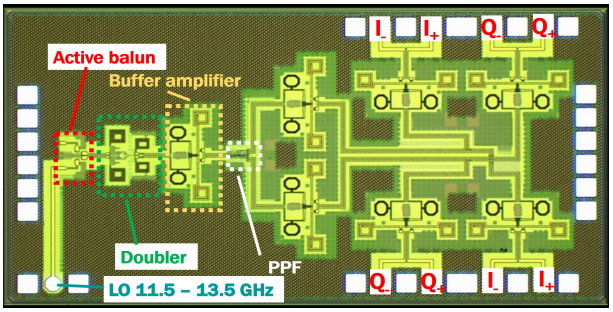


Fig. 4. Micrograph of the designed quadrature LO chain.

buffers are instantiated as shown in Fig. 1. The balun, shown in Fig. 3(a), is made of an input common-emitter (CE) and a common-base (CB) amplifier [6]. The CE is responsible for amplifying the input signal and feeding the CB amplifier through its emitter. It is important to notice that the impedance of the current source should be as high as possible to avoid signal leakage to ground. In fact, the voltage wave must reach the CB input and be amplified correctly. The single-ended output amplitude is $aV_{\text{in}}$, where $a = 0.5R_2/r_{\text{e}}$ and $r_{\text{e}}$ is the emitter resistance [6]. Fig. 3(b) shows the schematic of the buffer amplifier. This amplifier allows for a robust differential output because it is designed to enhance the common-mode rejection ratio ($CMRR$). A capacitance is added, not shown in the schematic, on the base of $Q_1$ to enhance the $CMRR$. Indeed,

$$CMRR = 1 + 2g_{\text{m}}R_{\text{oQ1}}\,, \quad (3)$$

where $R_{\text{oQ}_1}$ is the output resistance of $Q_1$ [7]. As shown in Fig. 3(b), the input matching network (IMN) consists of a series inductor, $L_1$, and a DC-block capacitor, $C_1$, while the output matching network (OMN) is based on a shunt inductor, $L_2$, and a series capacitor, $C_2$. For simplicity, the biasing networks are not shown. Fig. 3(c) shows the schematic of the doubler. This circuit is responsible for doubling the low-frequency LO. It is made of a Gilbert-cell, where the $\lambda/4$ delay line among the top quad and bottom differential pair sections is avoided to lower the area occupation [8]. According to

$$\cos(\alpha)\cos(\alpha) = 0.5[1 - \cos(2\alpha)]\,, \quad (4)$$

multiplying the same signal results in a DC term which is blocked by means of $C_{2\text{a}}$ in Fig. 3(c). However, the ideality of the differential signal is restored by the buffer amplifier, as already mentioned. The IMN consists of a series capacitor, $C$, and a shunt inductor, $L_1$, whereas $C_{1\text{a}}$ and $C_{1\text{b}}$ are used both as part of the IMN and as DC-block. Moreover, the OMN is designed using shunt inductors, $L_2$, series capacitors, $C_{2\text{a}}$, and shunt capacitors, $C_{2\text{b}}$, in Fig. 3(c). The PPF is presented in Fig. 3(d). It is a symmetric network composed of resistors and capacitors [9]. Two resonant frequencies, $f_1 = 1/2\pi R_1C$ and $f_2 = 1/2\pi R_2C$, are chosen as discussed in the previous section changing the resistor values. The quadrature filter presents two stages to have the same bandwidth of [10] while achieving better performance to load variations, which is relevant for a correct image-rejection.

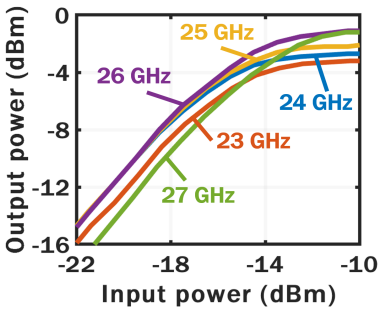


Fig. 5. Measured power of a single-ended output across input power.

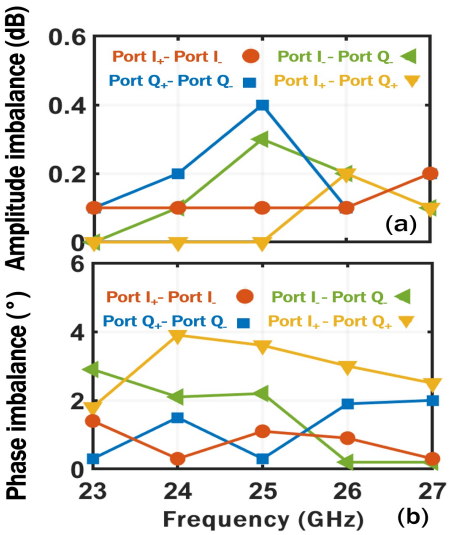


Fig. 6. Measured (a) amplitude and (b) phase imbalance across frequency.

## IV. Measurement Results

The LO chain is fabricated using the IHP SG13S technology. It features five thin metal layers and two thick top ones devoted to high-frequency passives. The chip is shown in Fig. 4 and occupies $2 \times 0.85\,\mathrm{mm}^2$, excluding the pads. Instead, Continuos-wave (CW) measurements are carried out using a signal generator and a spectrum analyzer, while the conversion phase is measured using a ZNA43 from R&S®. In Fig. 5, the power of a single-ended output is plotted across the input power. The LO chain achieves a maximum saturated power ($P_{sat}$) of $-1\,\mathrm{dBm}$ at 26 GHz. However, the $P_{sat}$ stays above $-3.2\,\mathrm{dBm}$ for the band of interest. Fig. 6 reports the imbalance between the four different output ports. These ports are considered for I and Q, adding a subscript symbol to distinguish between the positive and the negative output. Fig. 6(a) shows that the maximum gain imbalance is $0.4\,\mathrm{dB}$ at 25 GHz, while the phase imbalance is reported in Fig. 6(b). Here, the phase imbalance is always lower than $4°$. According to the previous analysis, this LO chain allows an $IMRR$ always better than $30\,\mathrm{dB}$. Finally, the performance summary and the state-of-the-art comparison are reported in Table I.

TABLE I
Performance summary and state-of-the-art comparison

| | Tech. | Freq. | $P_{sat}$ | Ampl. im. | Ph. im. |
|---|---|---|---|---|---|
| Unit | - | (GHz) | (dBm) | (dB) | (°) |
| [1] | 65-nm CMOS | 20 to 23 | -10 | - | - |
| [2] | 28-nm CMOS | 19 to 28 | - | 0.1* | 0.4* |
| [3] | 180-nm SiGe | 20 to 28 | -5 to 0 | no I/Q | no I/Q |
| This work | 130-nm SiGe | 23 to 27 | -3.2 to -1 | 0.4 | 3.9 |

* simulated

## V. Conclusion

An LO chain for sideband-suppression/image-rejection up-/down-converter is reported. The circuit is suitable for 5G mm-wave applications and has quadrature capabilities to feed mixers of the transmitting and receiving paths. The LO achieves low phase and amplitude imbalance, resulting in an optimal circuit for upconverters which suppress the lower sideband and downconverters with image-rejection capabilities. Finally, the analysis shows that this LO chain allows an $IMRR$ always better than $30\,\mathrm{dB}$.

## Acknowledgment

The authors thank Mr Thomas Mausolf for the help with the measurements, Mr Dieter Ferling for his support, Mr Bernd Gruber for the valuable discussions, and IHP for the chip production.

## References

[1] H. Nam *et al.*, "A Compact I/Q Upconversion Chain for a 5G Wireless Transmitter in 65-nm CMOS Technology," *IEEE Microwave and Wireless Components Letters*, vol. 30, no. 3, pp. 284–287, 2020.

[2] F. Quadrelli *et al.*, "A Broadband 22-31-GHz Bidirectional Image-Reject Up/Down Converter Module in 28-nm CMOS for 5G Communications," *IEEE Journal of Solid-State Circuits*, vol. 57, no. 7, pp. 1968–1981, 2022.

[3] K. Kibaroglu, M. Sayginer, and G. M. Rebeiz, "A 28 GHz transceiver chip for 5G beamforming data links in SiGe BiCMOS," in *2017 IEEE Bipolar/BiCMOS Circuits and Technology Meeting (BCTM)*, 2017, pp. 74–77.

[4] S. Kulkarni, D. Zhao, and P. Reynaert, "Design of an optimal layout polyphase filter for millimeter-wave quadrature LO generation," *IEEE Transactions on Circuits and Systems II: Express Briefs*, vol. 60, no. 4, pp. 202–206, 2013.

[5] J. Kaukovuori *et al.*, "Analysis and Design of Passive Polyphase Filters," *IEEE Transactions on Circuits and Systems I: Regular Papers*, vol. 55, no. 10, pp. 3023–3037, 2008.

[6] A. Franzese *et al.*, "Ultra Broadband Low-Power 70 GHz Active Balun in 130-nm SiGe BiCMOS," in *2020 IEEE BiCMOS and Compound Semiconductor Integrated Circuits and Technology Symposium (BCICTS)*, 2020, pp. 1–4.

[7] P. R. Gray *et al.*, *Analysis and design of analog integrated circuits*. John Wiley & Sons, 2009.

[8] H. P. Forstner *et al.*, "Frequency quadruplers for a 77GHz subharmonically pumped automotive radar transceiver in SiGe," in *2009 European Microwave Integrated Circuits Conference (EuMIC)*, 2009, pp. 188–191.

[9] F. Behbahani *et al.*, "Cmos mixers and polyphase filters for large image rejection," *IEEE Journal of solid-state circuits*, vol. 36, no. 6, pp. 873–887, 2001.

[10] S. Y. Kim *et al.*, "An improved wideband all-pass I/Q network for millimeter-wave phase shifters," *IEEE transactions on microwave theory and techniques*, vol. 60, no. 11, pp. 3431–3439, 2012.